ORIGINAL PAPER

Nuclear targeting with cell-specific multifunctional tricarbonyl M(I) (M is Re, ^{99m}Tc) complexes: synthesis, characterization, and cell studies

Teresa Esteves · Fernanda Marques ·
António Paulo · José Rino · Prasant Nanda ·
C. Jeffrey Smith · Isabel Santos

Abstract Auger-emitting radionuclides such as ^{99m}Tc have been the focus of recent studies aiming at finding more selective therapeutic approaches. To explore the potential usefulness of ^{99m}Tc as an Auger emitter, we have synthesized and biologically evaluated novel multifunctional structures comprising (1) a pyrazolyl-diamine framework bearing a set of donor atoms to stabilize the $[M(CO)_3]^+$ (M is Re, ^{99m}Tc) core; (2) a DNA intercalating moiety of the acridine orange type to ensure close proximity of the radionuclide to DNA and to follow the internalization and subcellular trafficking of the compounds by confocal fluorescence microscopy; and (3) a bombesin (BBN) analogue of the type X-BBN[7-14] (where X is SGS, GGG) to provide specificity towards cells expressing the gastrin releasing peptide receptor (GRPr). Of the evaluated ^{99m}Tc complexes, **Tc^3** containing the GGG-BBN[7-14] peptide showed the highest cellular internalization in GRPr-positive PC3 human prostate tumor cells, presenting a remarkably high nuclear uptake in the same cell line. Live-cell confocal imaging microscopy studies with the congener Re complex, **Re^3**, showed a considerable accumulation of fluorescence in the nucleus, with kinetics of uptake similar to that exhibited by **Tc^3**. Together, these data show that the acridine orange intercalator and the metal fragment are colocalized in the nucleus, which indicates that they remain connected despite the lysosomal degradation of **Tc^3/Re^3**. These compounds are the first examples of ^{99m}Tc bioconjugates that combine specific cell targeting with nuclear internalization, a crucial issue to explore use of ^{99m}Tc in Auger therapy.

Keywords Rhenium · Technetium-99m · Tricarbonyl · DNA intercalator · Bombesin analogues

T. Esteves · F. Marques · A. Paulo · I. Santos (✉)
Unidade de Ciências Químicas e Radiofarmacêuticas,
Instituto Tecnológico e Nuclear,
Estrada Nacional 10,
2686-953 Sacavém, Portugal
e-mail: isantos@itn.pt

J. Rino
Instituto de Medicina Molecular,
Faculdade de Medicina da Universidade de Lisboa,
Av. Prof. Egas Moniz,
1649-028 Lisbon, Portugal

P. Nanda · C. J. Smith
Department of Radiology,
School of Medicine,
University of Missouri,
Columbia, MO 65212, USA

Introduction

Several therapeutic methods for treatment of tumors have emerged over time, but there is still an intense research effort to find more selective therapies providing the means of treating damaged tissues while sparing those that are healthy. Of such methods, targeted radionuclide therapy, which relies on the specific delivery of high doses of radiation to neoplastic tissues, is assuming increasing relevance. Different approaches are being explored to improve the selectivity of targeted radionuclide therapy, namely, those based on the use of Auger electron emitting radioisotopes. Owing to the very short range of these particles, the Auger electron emitter must reach the nucleus of target cells in close proximity to DNA. In this way, an enhanced therapeutic effect is obtained, causing little damage to nontarget tissues [1]. Among the existing Auger

emitting radionuclides, ^{125}I ($t_{1/2}$ of 60 days) and ^{111}In ($t_{1/2}$ of 2.8 days) have become two isotopes of interest owing to their yield of 21 and 14 Auger electrons per decay, respectively [2, 3]. Several studies have demonstrated the ability of these radionuclides to induce damage to DNA, namely, by formation of single-strand and double-strand breaks caused directly by the Auger electrons or by the action of reactive oxygen species [4–8].

^{99m}Tc ($t_{1/2}$ of 6.02 h) is a γ-emitter extensively used in nuclear medicine for early detection of several malignancies. This radionuclide is also an Auger emitter (four Auger electrons per decay) and its potential in Auger therapy began to be investigated recently [9–13]. For example, Häfliger et al. [9] and Agorastos et al. [10] have demonstrated the ability of ^{99m}Tc to induce double-strand breaks in DNA and have proved that the use of ^{99m}Tc complexes bearing DNA intercalating moieties can be a useful strategy to improve such ability, by favoring close proximity of the radionuclide to DNA. The same research group has synthesized and evaluated trifunctional M(I) (M is Re, ^{99m}Tc) tricarbonyl complexes of the [2+1] type, bearing a bombesin (BBN) analogue and a DNA intercalator. For the Re complexes, fluorescence microscopy studies using human tumor cells have shown a rapid and specific internalization into the cytoplasm but poor uptake in the nucleus [10, 11].

Regarding our interest on radioactive metal-based compounds for nuclear targeting, we have reported on $^{99m}Tc(I)$ tricarbonyl complexes stabilized by a pyrazolyl-diamine framework containing DNA intercalators of the anthracene and acridine type [14–16]. We found that the complexes bearing an anthracene derivative possess enhanced ability to induce cell death [14, 15]. On the other hand, compounds with an acridine orange (AO) derivative (Fig. 1) showed an increased ability to interact closely with DNA by intercalation while retaining the capability to target the nucleus of murine tumor cells [16].

Following our previous work and looking to introduce biological specificity towards specific cancer cell lines, we have designed trifunctional nuclear targeting structures based on Re and ^{99m}Tc complexes containing a pyrazolyl-diamine framework functionalized with a DNA intercalator and with a BBN peptide analogue as a biologically active targeting vector. BBN is a tetradecapeptide with high affinity for the gastrin releasing peptide receptor (GRPr) and is expressed in very high numbers in several tumor cells, such as prostate, breast, pancreatic, and small-cell lung cancer cells [17]. In this work, we used the analogue BBN[7-14] (Q-W-A-V-G-H-L-M-NH_2), having the W-A-V-G-H-L-M sequence which is directly involved in the binding to the GRPr and which should, therefore, carry the radionuclide to GRPr-positive tumoral tissues.

Herein we describe the synthesis of pyrazolyl-diamine chelators bearing AO as a DNA intercalating moiety and BBN analogues of the type X–BBN[7-14] (X is SGS and GGG) for specific cell targeting. The synthesis of the corresponding Re and ^{99m}Tc complexes, as well as their biological evaluation, is also described.

Materials and methods

All chemicals were of reagent grade. Solvents were dried and distilled prior to use according to described procedures [18]. Unless otherwise stated, the syntheses of the ligands and complexes were performed under a nitrogen atmosphere, using standard Schlenk techniques and dry solvents; the work-up procedures were performed under air. The starting material fac-[Re(H_2O)$_3$(CO)$_3$]Br was synthesized by the literature method [19]. Benzyl 2-(1-(2-bromoethyl)-3,5-dimethylpyrazol) acetate (1) and 10-(4-aminobutyl)-3,6-bis(dimethylamino)acridinium (6) were synthesized according to published methods [16, 20]. Rink amide 4-methylbenzhydrylalanine (MBHA) resin (0.64 mmol g^{-1}; 100–200 mesh) was from NovaBiochem (Merck, Germany). All the 9-fluorenylmethyloxycarbonyl (Fmoc)-protected amino acids were from CEM (Matthews, NC, USA). Na[$^{99m}TcO_4$] was eluted from a commercial $^{99}Mo/^{99m}Tc$ generator, using 0.9% saline. ^1H and ^{13}C NMR spectra were recorded using a Varian Unity 300 MHz spectrometer; ^1H and ^{13}C chemical shifts are given in parts per million and were referenced with the residual solvent resonances relative to SiMe$_4$. The NMR samples were prepared in CDCl$_3$ or CD$_3$OD. J values are given in hertz. IR spectra were recorded in the range 4,000–200 cm^{-1} as KBr pellets with a Bruker Tensor 27 spectrometer. Electrospray ionization mass spectrometry (ESI–MS) was performed using a Bruker HCT electrospray ionization quadrupole ion trap mass spectrometer. Elemental analyses were performed with a PerkinElmer automatic analyzer. Thin-layer chromatography (TLC) was done on Merck silica gel 60 F254 plates. Column chromatography was performed with silica gel 60 (Merck). High-performance liquid chromatography
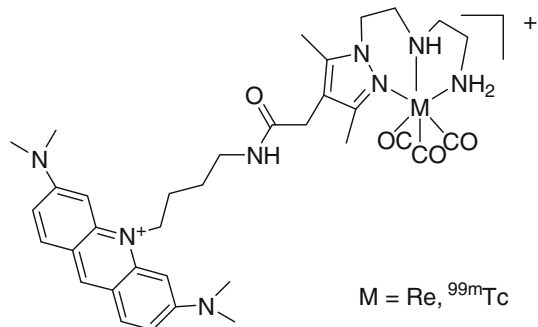

Fig. 1 Molecular structure of **Re-AO** and **^{99m}Tc-AO** complexes, where AO is acridine orange

(HPLC) analysis and purification of the ligands and Re and ^{99m}Tc complexes were performed with a PerkinElmer LC pump 200 coupled to an LC 290 tunable UV–vis detector and to a Berthold LB-507A radiometric detector using an analytic Macherey–Nagel C_{18} reversed-phase column (Nucleosil 100-5, 250 mm × 4 mm) with a flow rate of 1.0 mL min^{-1}; UV detection, 280 nm; eluents, A—aqueous 0.1% CF_3CO_2H solution, B—acetonitrile modified with 0.1% CF_3CO_2H; method: 0–3 min, 100% eluent A; 3–3.1 min, 100–75% eluent A; 3.1–9 min, 75% eluent A; 9–9.1 min 75–66% eluent A; 9.1–53 min, 66–10% eluent A; 53–55 min, 10% eluent A. Radioactivity measurements were done using an Aloka ionization chamber, an IGC-3 curiemeter, or a Berthold LB 2111 γ-counter.

Synthesis of the bifunctional ligand **L^1** and the respective Re complex **Re^1**

Benzyl 2-(1-(2-(2-(tert-butoxycarbonylamino) ethylamino)ethyl)-3,5-dimethyl-1H-pyrazol-4-yl) acetate

Benzyl 2-(1-(2-bromoethyl)-3,5-dimethylpyrazol) acetate (**1**) (4.543 g, 12.93 mmol) dissolved in CH_3CN (45 mL) was added dropwise to a mixture of N-boc-1,2-aminoethane (boc is tert-butoxycarbonyl; 4.144 g, 25.86 mmol), K_2CO_3 (3.575 g, 25.86 mmol), and KI (0.107 g, 0.65 mmol) in CH_3CN (50 mL). The resulting mixture was refluxed overnight, filtered, and the residue that was obtained was purified by column chromatography using a gradient elution from hexane/AcOEt (50:50) to 100% AcOEt followed by a gradient elution from 100% $CHCl_3$ to MeOH/$CHCl_3$ (90:10), to give benzyl 2-(1-(2-(2-(tert-butoxycarbonylamino)ethylamino)ethyl)-3,5-dimethyl-1H-pyrazol-4-yl) acetate (**2**) (4.942 g, 89%) as a dark-brown oil. ^{1}H(300 MHz; $CDCl_3$; Me$_4$Si): 1.29 (9H, s, 3CH$_3$), 2.03 (6H, s, 2CH$_3$), 2.56 (2H, t, J 5.7, CH$_2$), 2.84 (2H, t, J 6.0, CH$_2$), 3.04 (2H, m, CH$_2$), 3.25 (2H, s, CH$_2$), 3.91 (2H, t, J 6.0, CH$_2$), 4.96 (2H, s, CH$_2$), 5.37 (1H, s br, NH), 7.16 (5H, m, 5CH-Ar). ^{13}C NMR (Table S3).

Ethyl 4-((2-(4-(2-(benxyloxy)-2-oxoethyl)-3,5-dimethylpyrazol)ethyl)(2-(tert-butoxycarbonylamino) ethyl)amino) butanoate

Et$_3$N (8.4 mL, 60.56 mmol) and NaI (0.076 g, 0.51 mmol) were added to compound **2** (4.346 g, 10.09 mmol), which was dissolved in CH_3CN (20 mL). Ethyl 4-bromobutyrate (4.3 mL, 30.28 mmol), in CH_3CN (15 mL), was added dropwise to the previous suspension and the mixture was refluxed for 48 h. Then, the suspension was filtered and the organic solvent was removed under reduced pressure. The resulting residue was extracted with CH_2Cl_2 and water. The organic phase was dried over MgSO$_4$, the solvent was removed under reduced pressured, and the product was

purified by column chromatography, using a gradient elution from 100% $CHCl_3$ to 100% MeOH, to give ethyl 4-((2-(4-(2-(benxyloxy)-2-oxoethyl)-3,5-dimethylpyrazol)ethyl) (2-(tert-butoxycarbonylamino)ethyl)amino) butanoate (**3**) (2.909 g, 53%) as a light-yellow oil. ^{1}H(300 MHz; $CDCl_3$; Me$_4$Si): 1.16 (3H, t, J 6.9, CH$_3$), 1.36 (9H, s, 3CH$_3$, boc), 1.55 (2H, quintuplet, J 6.6 and J 7.2, CH$_2$), 2.10 (8H, m, 2CH$_3$, CH$_2$), 2.36 (2H, t, J 6.9, CH$_2$), 2.42 (2H, t, J 6.0, CH$_2$), 2.68 (2H, t, J 6.3, CH$_2$), 2.99 (2H, m, CH$_2$), 3.30 (2H, s, CH$_2$), 3.91 (2H, t, J 6.3, CH$_2$), 4.03 (4H, q, J 6.9 and J 7.2, 2CH$_2$), 5.02 (2H, s, CH$_2$), 5.32 (1H, s br, NH), 7.24 (5H, m, 5CH-Ar). ^{13}C NMR (Table S3).

2-(1-(2-((2-(tert-Butoxycarbonylamino)ethyl)(4-ethoxy-4-oxobutyl)amino)ethyl)-3,5-dimethylpyrazol) acetic acid

Compound **3** (0.084 g, 0.15 mmol) and approximately 500 mg of Pd on activated carbon (10% Pd) were suspended in EtOH (25 mL). H$_2$ was bubbled through the solution during the day and the solution was kept saturated overnight. The suspension was filtered over Celite and the solvent was removed under reduced pressure to give 2-(1-(2-((2-(tert-butoxycarbonylamino)ethyl)(4-ethoxy-4-oxobutyl)amino) ethyl)-3,5-dimethylpyrazol) acetic acid (**4**) (0.061 g, 87%) as a yellow oil. ^{1}H(300 MHz; $CDCl_3$; Me$_4$Si): 1.00 (3H, t, J 7.2, CH$_3$), 1.19 (9H, s, 3CH$_3$, boc), 1.44 (2H, m, CH$_2$), 1.95 (8H, m, 2CH$_3$, CH$_2$), 2.29 (4H, m, 2CH$_2$), 2.58 (2H, m, CH$_2$), 2.86 (2H, m, CH$_2$), 3.06 (2H, s, CH$_2$), 3.85 (4H, m, 2CH$_2$), 5.26 (1H, s br, NH). ^{13}C NMR (Table S3).

Ethyl 4-((2-(tert-butoxycarbonylamino)ethyl)(2-(4-(2-(2,5-dioxopyrrolidinyloxy)-2-oxoethyl)-3,5-dimethylpyrazol) ethyl)amino) butanoate

N-hydroxysuccinimide (NHS; 0.017 g, 0.15 mmol) was added to a solution of compound **4** (0.061 g, 0.13 mmol) in CH_2Cl_2 (20 mL) in an ice bath and the mixture was stirred for 30 min. Then, 1-ethyl-3-(3-dimethylaminopropyl) carbodiimide (0.028 g, 0.15 mmol) was added and the reaction mixture was stirred for an additional 48 h at room temperature. The solvent was removed under reduced pressure and the resulting solid was extracted with CH_2Cl_2, dried over MgSO$_4$, and the solvent was removed under reduced pressure to give ethyl 4-((2-(tert-butoxycarbonylamino)ethyl)(2-(4-(2-(2,5-dioxopyrrolidinyloxy)-2-oxoethyl)-3,5-dimethylpyrazol)ethyl)amino) butanoate (**5**) (0.052 g, 71%) as a yellow oil. ^{1}H(300 MHz; $CDCl_3$; Me$_4$Si): 1.11 (3H, t, J 6.9, CH$_3$), 1.31 (9H, s, 3CH$_3$, boc), 1.47 (2H, m, CH$_2$), 2.00 (2H, m, CH$_2$), 2.09 (3H, s, CH$_3$), 2.10 (3H, s, CH$_3$), 2.30 (2H, m, CH$_2$), 2.38 (2H, m, CH$_2$), 2.66 (6H, m, 2CH$_2$-NHS, CH$_2$), 2.94 (2H, m, CH$_2$), 3.51 (2H, s, CH$_2$), 3.88 (2H, m, CH$_2$), 3.96 (2H, q, J 7.2 and J 6.9, CH$_2$), 5.39 (1H, s br, NH). ^{13}C NMR (Table S3).

Ethyl 4-((2-(4-(2-(10-(4-butylamino)-3,6-bis(dimethylamino)acridinium)-2-oxoethyl)-3,5-dimethylpyrazol)ethyl)(2-(tert-butoxycarbonylamino)ethyl)amino) butanoate

A solution of **5** (0.829 g, 1.50 mmol) in dimethylformamide (DMF; 20 mL) was added to a solution of 10-(4-aminobutyl)-3,6-bis(dimethylamino)acridinium (**6**) (0.659 g, 1.58 mmol) and *N,N′*-diisopropylethylamine (DIPEA; 275 μL, 1.58 mmol) in DMF (30 mL) with stirring (1.5 h). After the mixture had been at room temperature for 3 days, the solvent was removed under reduced pressure and the residue was purified by column chromatography, using a gradient elution from CHCl$_3$/MeOH (95:5) to CHCl$_3$/MeOH/NH$_4$OH 25% (5:85:10), to give ethyl 4-((2-(4-(2-(10-(4-butylamino)-3,6-bis(dimethylamino)acridinium)-2-oxoethyl)-3,5-dimethylpyrazol)ethyl)(2-(*tert*-butoxycarbonylamino)ethyl)amino) butanoate (**7**) (0.211 g, 90%) as a red-orange solid. ^{1}H(300 MHz; CD$_3$OD; Me$_4$Si): 1.24 (3H, t, *J* 3.9, CH$_3$), 1.41 (9H, s, 3CH$_3$, boc), 1.61 (2H, m, CH$_2$), 1.83 (4H, m, 2CH$_2$), 2.05 (3H, s, CH$_3$), 2.17 (3H, s, CH$_3$), 2.19 (2H, m, CH$_2$), 2.47 (2H, t, *J* 7.2, CH$_2$), 2.53 (2H, t, *J* 6.3, CH$_2$), 2.75 (2H, t, *J* 6.6, CH$_2$), 3.03 (4H, t, *J* 6.3, 2CH$_2$), 3.26 (12H, s, 4CH$_3$), 3.32 (2H, m, CH$_2$), 3.98 (2H, t, *J* 6.3, CH$_2$), 4.08 (2H, q, *J* 7.2 and *J* 6.9, CH$_2$), 4.57 (2H, m, CH$_2$), 6.46 (2H, s, 2CH-Ar), 7.12 (2H, dd, *J* 2.1, *J* 1.8 and *J* 9.3, 2CH-Ar), 7.75 (2H, d, *J* 9.3, 2CH-Ar), 8.48 (1H, s, CH-Ar). ^{13}C NMR (Table S3). t_R = 16.95 min (100-5 C$_{18}$, 1.0 mL min^{-1}).

4-((2-(4-(2-(10-4-(Butylamino)-3,6-bis(dimethylamino)acridinium)-2-oxoethyl)-3,5-dimethylpyrazol)ethyl)(2-(tert-butoxycarbonylamino)ethyl)amino) butanoic acid

A solution of NaOH (0.090 g, 2.25 mmol) in water (2 mL) was added to a solution of **7** (0.240 g, 0.28 mmol) in water (13 mL) and the mixture was refluxed overnight. The mixture was filtered and the filtrate was neutralized with 3 M HCl. The solvent was removed under reduced pressure, the product was redissolved in CH$_2$Cl$_2$, and the salts were centrifuged and separated and the solvent was removed again under reduced pressure to give 4-((2-(4-(2-(10-4-(butylamino)-3,6-bis(dimethylamino)acridinium)-2-oxoethyl)-3,5-dimethylpyrazol)ethyl) (2-(*tert*-butoxycarbonylamino)ethyl)amino) butanoic acid (**8**) (0.211 g, 91%) as an orange solid. ^{1}H(300 MHz; CD$_3$OD; Me$_4$Si): 1.40 (9H, s, 3CH$_3$, boc), 1.64 (2H, t, *J* 6.9, CH$_2$), 1.80 (4H, m, 2CH$_2$), 2.05 (3H, s, CH$_3$), 2.14 (5H, m, CH$_3$, CH$_2$), 2.46 (4H, m, 2CH$_2$), 2.71 (2H, t, *J* 6.3, CH$_2$), 2.98 (2H, m, CH$_2$), 3.24 (16H, m, 4CH$_3$, 2CH$_2$), 3.95 (2H, t, *J* 6.3, CH$_2$), 4.47 (2H, m, CH$_2$), 6.35 (2H, s, 2CH-Ar), 7.05 (2H, dd, *J* 1.8 and *J* 9.3, 2CH-Ar), 7.67 (2H, d, *J* 9.3, 2CH-Ar), 8.37 (1H, s, CH-Ar). ^{13}C NMR (Table S3). t_R = 16.38 min (100-5 C$_{18}$, 1.0 mL min^{-1}). *m/z* (ESI–MS): 745.3 [M]$^+$, 743.4 [M$^+$–2H]$^-$.

4-((2-(4-(2-(10-(4-Butylamino)-3,6-bis(dimethylamino)acridinium)-2-oxoethyl)-3,5-dimethylpyrazol)ethyl)(2-aminoethyl)amino) butanoic acid

A solution of **8** (0.211 g, 0.26 mmol) and trifluoroacetic acid (TFA; 2 mL, 25.96 mmol) in CH$_2$Cl$_2$ (2 mL) was stirred at room temperature overnight. Then, the solvent was removed under reduced pressure and the product was purified by column chromatography, using a gradient elution from 100% MeOH to 100% NH$_4$OH (25%), to give 4-((2-(4-(2-(10-(4-butylamino)-3,6-bis(dimethylamino)acridinium)-2-oxoethyl)-3,5-dimethylpyrazol)ethyl)(2-aminoethyl)amino) butanoic acid (**L^1**) [0.095 g (four TFA), 51%] as a red-orange solid. Found: C, 44.7; H, 4.1; N, 8.9. C$_{36}$H$_{53}$N$_8$O$_3$·4(CF$_3$CO$_2$H) requires C, 44.7; H, 4.9; N, 9.5%. ^{1}H(300 MHz; CD$_3$OD; Me$_4$Si): 1.88 (6H, m, 3CH$_2$), 2.09 (3H, s, CH$_3$), 2.20 (5H, m, CH$_2$, CH$_3$), 2.41 (2H, t, *J* 6.6, CH$_2$), 3.24 (16H, m, 4CH$_3$, 2CH$_2$), 3.41 (2H, t, *J* 5.4, CH$_2$), 3.51 (2H, m, CH$_2$), 3.60 (2H, t, *J* 5.4, CH$_2$), 4.42 (2H, t, *J* 5.7, CH$_2$), 4.51 (2H, t, *J* 6.0, CH$_2$), 6.42 (2H, s, 2CH-Ar), 7.09 (2H, dd, *J* 1.5 and *J* 9.3, 2CH-Ar), 7.70 (2H, d, *J* 9.3, 2CH-Ar), 8.39 (1H, s, CH-Ar). ^{13}C NMR (Table S3). t_R = 14.72 min (100-5 C$_{18}$, 1.0 mL min^{-1}). *m/z* (ESI–MS): 645.2 [M]$^+$.

fac-[Re(CO)$_3$(k^3-L^1)](CF$_3$CO$_2$)·3TFA

fac-[Re(CO)$_3$(k^3-L^1)](CF$_3$CO$_2$)·3TFA (**Re^1**) was obtained from the reaction of [Re(H$_2$O)$_3$(CO)$_3$]Br with an equimolar amount of **L^1** in refluxing H$_2$O (12 h) and was purified by reversed-phase HPLC (RP-HPLC; 34 mg, 56%) to give a red-orange solid. Found: C, 38.4; H, 3.7; N, 7.7. C$_{49}$H$_{56}$N$_8$F$_{15}$O$_{16}$Re requires C, 39.6; H, 3.8; N, 7.5%. ν_{max} (KBr) cm^{-1} (CO) 1,896, 2,026. ^{1}H(300 MHz; CD$_3$OD; Me$_4$Si): 1.88 (6H, m, 3CH$_2$), 2.27 (3H, s, CH$_3$), 2.34 (3H, s, CH$_3$), 2.43 (2H, t, *J* 6.9, CH$_2$), 2.68 (2H, m, 2CH), 2.76 (1H, m, CH), 2.88 (2H, m, 2CH), 3.28 (14H, m, 4CH$_3$, CH$_2$), 3.40 (2H, s, CH$_2$), 3.51 (2H, m, CH$_2$), 3.67 (1H, m, CH), 4.03 (1H, s br, NH), 4.20 (1H, m, CH), 4.51 (1H, m, CH), 4.61 (2H, t, *J* 6.6 and *J* 7.8, CH$_2$), 5.50 (1H, s br, NH), 6.51 (2H, s, 2CH-Ar), 7.15 (2H, dd, *J* 1.8 and *J* 9.3, 2CH-Ar), 7.79 (2H, d, *J* 9.3, 2CH-Ar), 8.51 (1H, s, CH-Ar). ^{13}C NMR (Table S3). t_R = 16.50 min (100-5 C$_{18}$, 1.0 mL min^{-1}). *m/z* (ESI–MS): 458.00 [M]$^{2+}$.

Peptide synthesis

Solid-phase peptide synthesis was performed with an automated peptide synthesizer (Liberty; CEM, Matthews, NC, USA) employing a standard Fmoc strategy [21]. BBN analogues **9** and **10** of the type X–BBN with the following general structure X-Q-W-A-V-G-H-L-M, where the spacer group X is SGS (**9**) or GGG (**10**), were assembled on a Rink amide 4-methylbenzhydrylalanine resin. After the

desired sequences of amino acids had been assembled, cleavage from the resin and simultaneous side chain deprotection of the peptides were accomplished by using a cleavage cocktail comprising TFA/thioanisole/H_2O/ethanedithiol (94:1:2.5:2.5) (% v/v). The crude peptides were purified by RP-HPLC. RP-HPLC analysis and purification of the peptide conjugates was performed as previously described [22].

Synthesis of the peptide conjugates L^2 and L^3

Intermediate 7 was coupled to the N-terminal of the BBN peptide analogues (2.5 equiv) using O-benzotriazole-N,N,N',N'-tetramethyluronium hexafluorophosphate (HBTU; 2.5 equiv) and DIPEA (4.6 equiv) for 2 h at room temperature. After purification by RP-HPLC and ESI–MS analysis, the boc protecting group of the intermediates, present on the terminal amine of the pyrazolyl-diamine framework, was removed using the method previously described. The resulting solutions were precipitated in Et_2O for 1 h in a freezer and washed five times with cold Et_2O. The resulting precipitates were dried, purified by RP-HPLC, and characterized by ESI–MS to yield the peptide conjugates L^2 and L^3. L^2: t_R = 17.52 min (100-5 C_{18}, 1.0 mL min^{-1}). m/z (ESI–MS, $C_{87}H_{129}N_{24}O_{16}S^+$): 600.3 $[M+2H]^{3+}$, 900.1 $[M+H]^{2+}$. L^3: t_R = 17.22 min (100-5 C_{18}, 1.0 mL min^{-1}). m/z (ESI–MS, $C_{85}H_{125}N_{24}O_{14}S^+$): 580.4 $[M+2H]^{3+}$, 869.8 $[M+H]^{2+}$.

The side products L^4 and L^5 were isolated during the purification of L^2 and L^3, respectively. L^4 and L^5 were characterized by ESI–MS and HPLC. L^4: t_R = 16.63 min (100-5 C_{18}, 1.0 mL min^{-1}). m/z (ESI–MS, $C_{87}H_{129}N_{24}O_{17}S^+$): 605.7 $[M+2H]^{3+}$, 908.0 $[M+H]^{2+}$. L^5: t_R = 16.54 min (100-5 C_{18}, 1.0 mL min^{-1}). m/z (ESI–MS, $C_{85}H_{125}N_{24}O_{15}S^+$): 585.8 $[M+2H]^{3+}$, 878.1 $[M+H]^{2+}$.

Synthesis of Re(I) conjugates Re^2 and Re^3

The complex Re^1 (2.5 equiv) was coupled to the N-terminal of the BBN peptide analogues 9 and 10 using HBTU (2.5 equiv) and DIPEA (4.6 equiv) for 2 h at room temperature. The resulting solutions were precipitated in Et_2O for 1 h in a freezer and washed five times with cold Et_2O. The resulting precipitates were purified by RP-HPLC and characterized by ESI–MS as Re^2 and Re^3. Re^2: t_R = 20.48 min (100-5 C_{18}, 1.0 mL min^{-1}). m/z (ESI–MS, $C_{90}H_{129}N_{24}O_{19}SRe^{2+}$): 690.1 $[M+H]^{3+}$, 1,034.5 $[M]^{2+}$. Re^3: t_R = 20.63 min (100-5 C_{18}, 1.0 mL min^{-1}). m/z (ESI–MS, $C_{88}H_{125}N_{24}O_{17}SRe^{2+}$): 670.3 $[M+H]^{3+}$, 1,004.7 $[M]^{2+}$.

During purification, complexes Re^4 and Re^5 were also isolated and characterized by ESI–MS. Re^4: t_R = 19.00 min (100-5 C_{18}, 1.0 mL min^{-1}). m/z (ESI–MS, $C_{90}H_{129}N_{24}O_{20}$

SRe^{2+}): 695.9 $[M+H]^{3+}$, 1,043.0 $[M]^{2+}$. Re^5: t_R = 20.04 min (100-5 C_{18}, 1.0 mL min^{-1}). m/z (ESI–MS, $C_{88}H_{125}N_{24}O_{18}SRe^{2+}$): 675.6 $[M+H]^{3+}$, 1,012.6 $[M]^{2+}$.

Synthesis of the $^{99m}Tc(I)$ complexes Tc^2–Tc^5

In a glass vial, 100 μL of a 10^{-5} M aqueous solution of the conjugates L^2–L^5 was added to 100 μL of the organometallic precursor fac-$[^{99m}Tc(CO)_3(H_2O)_3]^+$ (5–7 mCi) in saline at pH 7.4. The reaction mixture was heated to 100 °C for 30 min, cooled at room temperature, and the final solution was analyzed by RP-HPLC.

Partition coefficient measurements

The log $P_{o/w}$ values of complexes Tc^2–Tc^5 (Table S2) were determined by the "shake flask" method under physiological conditions [n-octanol/0.1 M phosphate-buffered saline (PBS), pH 7.4] [23]. The HPLC-purified compounds (100 μL, approximately 100 μCi) were added to a test tube containing 1 mL of n-octanol and 1 mL of a PBS solution. The tube was vortexed for 1 min and centrifuged for 5 min at 3,500 rpm. After centrifugation, 500 μL of the aqueous phase was transferred to another tube and further extracted with 500 μL of n-octanol, as described for the first extraction. After separation of the phases, 50-μL aliquots of each phase were taken for radioactivity measurement (in duplicate) using a γ-counter. The partition coefficient ($P_{o/w}$) was calculated on the basis of the ratio (activity in octanol layer)/(activity in aqueous layer) and is expressed as log $P_{o/w}$.

Cell studies

Cell culture

B16F1 murine melanoma cells and PC3 human prostate tumor cells were grown in Dulbecco's modified Eagle's (DMEM) containing GlutaMax I supplemented with 10% heat-inactivated fetal bovine serum and 1% penicillin/streptomycin antibiotic solution (all from Invitrogen) or RPMI supplemented with 10% heat-inactivated fetal bovine serum and 1% penicillin/streptomycin antibiotic solution (all from Gibco), respectively. Cells were cultured in a humidified atmosphere of 95% air and 5% CO_2 at 37 °C (Heraeus, Germany), with the medium changed every other day.

Confocal fluorescence microscopy

Cellular uptake of fluorescent Re compounds was visualized by performing time-lapse confocal microscopy imaging of live PC3 cells. Briefly, cells in medium were seeded on sterile 35-mm Petri dishes (MatTek, Ashland, MA,

USA) at a density of approximately 105 cells mL^{-1}. After 24 h incubation at 37 °C, the cells were labeled with dihydroethidium (Molecular Probes, Eugene, OR, USA) at 1 μg mL^{-1} for 20 min at 37 °C. Dihydroethidium is a neutral probe able to penetrate the cellular membrane of live cells. Once internalized, it is dehydrogenated (oxidized) to ethidium bromide [24]. After labeling, the cells were washed three times and maintained in DMEM/F12 without phenol red for live imaging experiments. Cells were imaged with a Zeiss LSM 510 META inverted laser scanning confocal microscope (Carl Zeiss, Germany) equipped with a large incubator for 37 °C temperature control (Pecon, Germany) using a PlanApochromat ×63/1.4 oil-immersion objective. Ethidium bromide fluorescence was detected using the 514-nm laser line of an Ar laser (45-mW nominal output) and a 615-nm long-pass filter. The fluorescence of Re compounds was detected using the 488-nm laser line of the same Ar laser and a 500–550-nm band-pass filter. The pinhole aperture was adjusted in both channels to achieve the same optical slice thickness (1 μm). After addition of a solution of 15 μM Re complexes to the cell medium, sequential images in both green (Re compound) and red (ethidium bromide) channels were then acquired every minute during a 1-h time period.

Stability in the cell culture medium by thin-layer chromatography

The stability in cell culture medium was examined by incubating the peptide radioconjugates (40 μL, 29 μCi) with PC3 or B16F1 cell medium at 37 °C. At appropriate time points (0, 1, and 3 h), aliquots were sampled by TLC using silica gel TLC strips (Polygram Sil G, Macherey–Nagel) developed with a mobile phase of 5% 6 N HCl in methanol. The radioactive distribution on the TLC strips was detected using a Berthold LB 505 detector coupled to a radiochromatogram scanner. The following R_f values were found for the different ^{99m}Tc complexes under study: 0.28 for **Tc^2**; 0.25 for **Tc^3**; 0.18 for **Tc^4**; 0.16 for **Tc^5**. Under the same chromatographic conditions, ^{99m}TcO$_4^-$ and the precursor [^{99m}Tc(CO)$_3$(H$_2$O)$_3$]$^+$ showed R_f values of 0.72 and 0.77, respectively.

Cellular uptake and retention

The cellular internalization assay was performed in B16F1 and PC3 cells seeded at a density of 2×10^5 cells per well in 24-well tissue culture plates and allowed to attach overnight. The cells were incubated at 37 °C for 5 min to 4 h with 200,000 cpm of the complex in 0.5 mL of assay medium [minimum essential medium with 25 mM N-(2-hydroxyethyl)piperazine-N'-ethanesulfonic acid and 0.2%

bovine serum albumin] as previously described [14]. The cellular retention of the internalized radioconjugate was determined by incubating cells with the radiolabeled compounds for 1 h at 37 °C, washing them with cold assay medium, removing the membrane-bound radioactivity with acid buffer wash, and monitoring the radioactivity release into the culture medium (0.5 mL) at 37 °C at different time points over a 4-h incubation period as previously described [16].
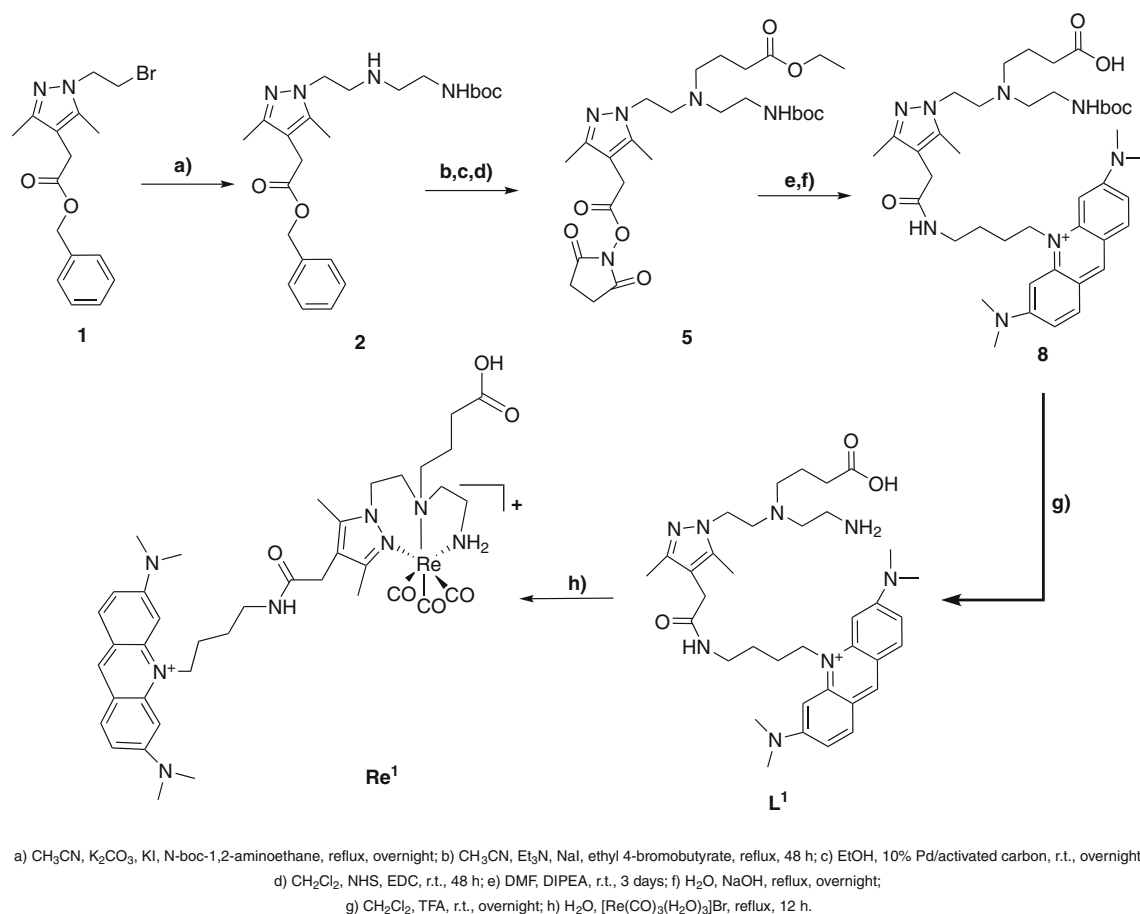
Nuclear uptake

B16F1and PC3 cells were seeded at a density of 0.2 million per well into 24-well tissue culture plates and allowed to attach overnight. The cells were incubated in humidified 5% CO$_2$/95% air at 37 °C for a period spanning from 5 min to 4 h with approximately 200,000 cpm of radioconjugate in 0.5 mL of assay medium. After incubation, the cells were treated according to a published method [16]. Briefly, the cells were lysed and the nucleus pellet was separated by centrifugation. The activities of the supernatant (activity outside the nucleus) and precipitate (activity retained in the nucleus) were measured (three replicates) with a γ-counter. The nuclear uptake was expressed as a percentage of the total activity added to the cells.

Results and discussion

The pyrazolyl-diamine framework acts as a tridentate ligand towards the *fac*-[M(CO)$_3$]$^+$ (M is Re, ^{99m}Tc) core, giving complexes with high stability in vitro and in vivo. As mentioned already, this framework was previously derivatized with an AO derivative that was introduced at the 4-position of the pyrazole ring without compromising its ability to intercalate into the DNA base pairs after coordination to the *fac*-[M(CO)$_3$]$^+$ core (Fig. 1) [16]. Therefore, the 4-position was also used in this study to introduce an intercalator of the AO type, and a pendant butyric arm was attached at the central amine of the chelating ligand framework and used for further coupling of the BBN peptide analogues.

As reported herein, the synthesis of Re/^{99m}Tc trifunctional complexes bearing the AO intercalator and the BBN peptides was performed using two strategies. In the case of Re, the trifunctional complexes were obtained via an intermediate complex bearing the AO fragment and a pendant butyric arm used to couple the bioactive peptide. By contrast, the ^{99m}Tc congeners were synthesized by reacting the *fac*-[^{99m}Tc(CO)$_3$(H$_2$O)$_3$]$^+$ precursor with the pyrazolyl-diamine ligands functionalized simultaneously with the DNA intercalator and the BBN analogues.

a) CH$_3$CN, K$_2$CO$_3$, KI, N-boc-1,2-aminoethane, reflux, overnight; b) CH$_3$CN, Et$_3$N, NaI, ethyl 4-bromobutyrate, reflux, 48 h; c) EtOH, 10% Pd/activated carbon, r.t., overnight;
d) CH$_2$Cl$_2$, NHS, EDC, r.t., 48 h; e) DMF, DIPEA, r.t., 3 days; f) H$_2$O, NaOH, reflux, overnight;
g) CH$_2$Cl$_2$, TFA, r.t., overnight; h) H$_2$O, [Re(CO)$_3$(H$_2$O)$_3$]Br, reflux, 12 h.

Scheme 1 Synthesis of **L^1** and the respective rhenium complex **Re^1**

Synthesis and characterization of bifunctional
pyrazolyl-diamine chelators bearing an AO intercalator
and the respective Re complex

The synthesis of the bifunctional chelator for further cou-
pling of the BBN analogues relied on the use of benzyl and
ethyl esters as orthogonal carboxylic protecting groups. As
shown in Scheme 1, the pyrazolyl-diamine derivative
benzyl 2-(1-(2-bromoethyl)-3,5-dimethylpyrazol) acetate
(**1**) was treated with *N*-boc-1,2-aminoethane in dry
CH$_3$CN, forming compound **2**, which was further reacted
with ethyl-4-bromobutyrate to afford ethyl 4-((2-(4-(2-
(benxyloxy)-2-oxoethyl)-3,5-dimethylpyrazol)ethyl)(2-
(*tert*-butoxycarbonylamino)ethyl)amino) butanoate (**3**).
The benzyl ester of **3** was selectively removed by a Pd/H$_2$
hydrogenation reaction and the resulting free carboxylate
group was activated with NHS, leading to compound **5**.
This activated ester was further reacted with 10-(4-amino-
butyl)-3,6-bis(dimethylamino)acridinium (**6**) in dry DMF
and in the presence of DIPEA, giving **8** after deprotection
of the ethyl ester with an aqueous solution of NaOH.
Removal of the boc-protecting group of **8** with TFA led to
L^1, which was isolated as a red-orange solid in 12% overall

yield after purification by HPLC. **L^1** has been fully char-
acterized by multinuclear NMR spectroscopy, ESI–MS,
and CHN analysis. As described herein, the boc–protected
L^1 (**8**) was used for conjugation to the BBN peptides
(Scheme 2) and **L^1** was used to prepare the **Re^1** complex.

The synthesis of the bifunctional Re complex (**Re^1**), to
be used for conjugation to X-BBN[7-14], was done by
ligand-exchange reaction of *fac*-[Re(H$_2$O)$_3$(CO)$_3$]Br with
L^1 (Scheme 1). **Re^1** was recovered as a red-orange solid
after HPLC purification. It is soluble in MeOH and mod-
erately soluble in water, being stable towards air oxidation
or hydrolysis. **Re^1** was fully characterized by IR spec-
troscopy, ^{1}H and ^{13}C NMR spectroscopy, ESI–MS, CHN
analysis, and HPLC. The IR spectrum of **Re^1** showed two
intense absorption bands centered at 1,896 and 2,026 cm^{-1}
that were assigned to the $v(C\equiv O)$ stretching modes of the
fac-[Re(CO)$_3$]$^+$ unit. These frequencies compare well with
the ones previously reported for other Re(I) tricarbonyl
complexes anchored by pyrazolyl-diamine chelators
[14–16, 22]. The ^{1}H NMR data obtained for **Re^1** corrob-
orated a facial coordination of the ligand through the pyr-
azolyl ring, the central nitrogen atom, and the terminal
amine group, as a set of multiplets for the diastereotopic
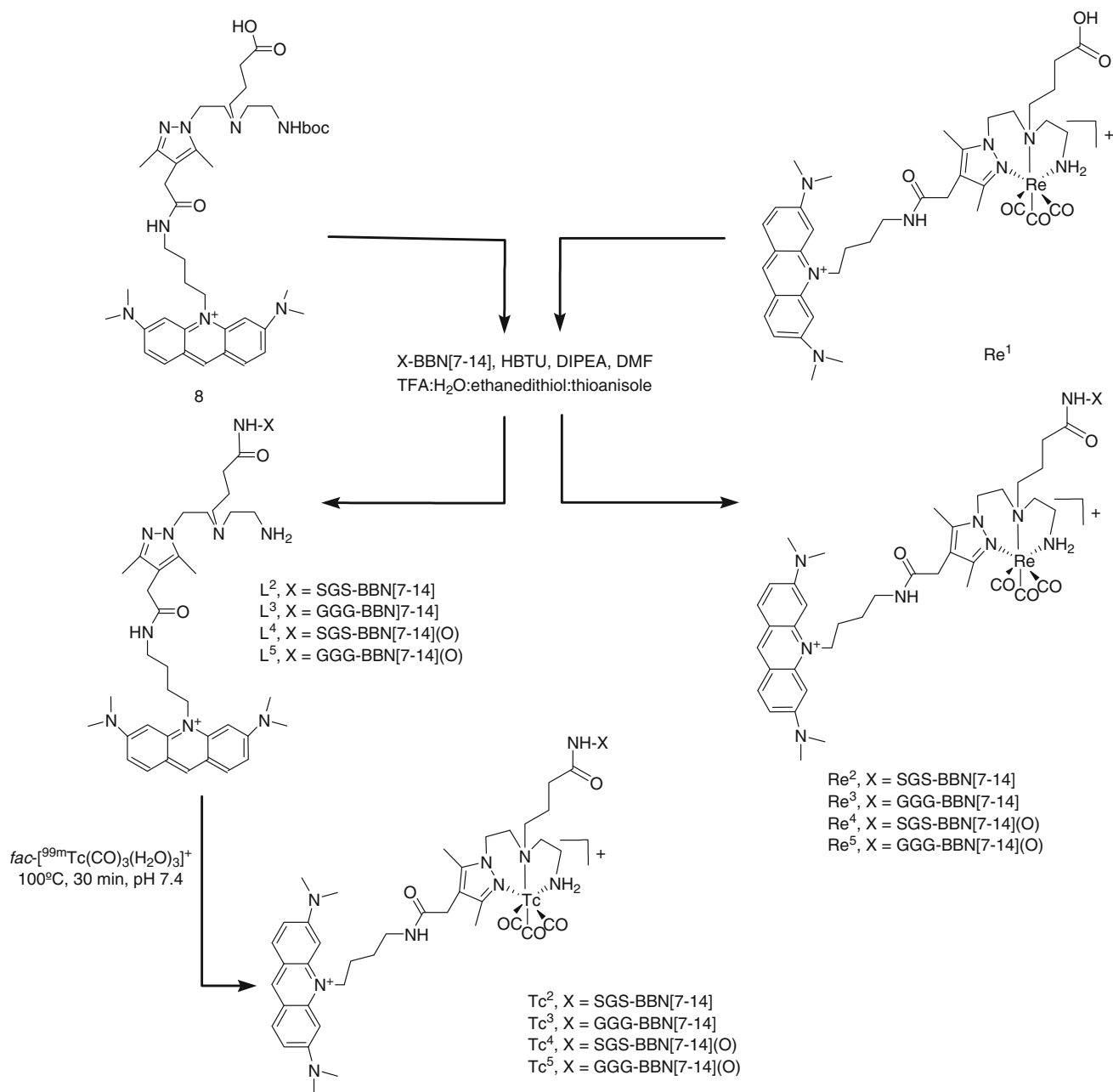
Scheme 2 Synthesis of the peptide conjugates (L^2–L^5), rhenium complexes (Re^2–Re^5), and technetium complexes (Tc^2–Tc^5)

methylenic protons of the pyrazolyl-diamine framework and for the –NH$_2$ protons were observed. Such multiplets exhibited chemical shifts significantly different from those of the corresponding protons in the respective free ligand L^1. In contrast, the signals due to the protons of the chromophore unit as well as those due to the protons from the butylenic and propylenic linkers showed a pattern and chemical shifts very similar to the ones found in the free ligand L^1. These findings confirmed that the chromophore unit and the propionic pendant arm were not interacting with the metal. In the positive mode, the ESI–MS spectrum

of Re^1 showed a prominent peak at *m/z* 458.00 corresponding to $[M]^{2+}$ with the correct isotope distribution pattern.

Conjugation of BBN analogues to the bifunctional chelator and to the respective Re complex

Two BBN analogues, SGS-BBN[7-14] (**9**) and GGG-BBN [7-14] (**10**), were prepared by solid-phase peptide synthesis using standard Fmoc chemistry in an automated synthesizer as previously described [22, 25]. The BBN analogues

were cleaved from the resin, purified by RP-HPLC, and characterized by ESI–MS to confirm their identity (Table S1).

As indicated in Scheme 2, BBN analogues **9** and **10** were conjugated in solution to compound **8**, affording compounds **L²** and **L³** after removal of the boc-protecting group. In a similar way, the conjugation of the same analogues to **Re¹** allowed the synthesis of the metallated peptides **Re²** and **Re³**.

During the conjugation reactions of **8** with **9** and **10**, the desired bioconjugates (**L²** and **L³**) were obtained along with another species showing a peak in the ESI–MS spectra with a difference of +16 Da relative to the experimental and calculated molecular ions of **L²** and **L³**. These findings indicated that the coupling of the BBN analogues to the bifunctional chelators was accompanied by some degree of oxidation. The corresponding Re complexes **Re²** and **Re³** also undergo a slow oxidation over time, but not during the conjugation reactions as described herein. The oxidized species (**L⁴**, **L⁵**, **Re⁴**, and **Re⁵**) were also isolated, as they could be efficiently separated from the nonoxidized products (**L²**, **L³**, **Re²**, and **Re³**) by RP-HPLC. We presume that the oxidation takes place on the methionine residue of the peptidic sequences since this amino acid is very prone to oxidation to a sulfoxide [26]. As discussed later, the in vitro biological evaluation of the ^{99m}Tc complexes of **L²**–**L⁵** seems to corroborate this possibility. The formulations of all compounds, oxidized and nonoxidized, were confirmed by ESI–MS (Fig. S1, Table S1).

Synthesis and characterization of ^{99m}Tc complexes

It is well accepted that modifications at position 14 occupied by methionine are an important factor in determining whether the binding affinity of the BBN sequence for the GRPr will or will not be affected [27–29]. Therefore, we elected to synthesize the ^{99m}Tc(I) tricarbonyl complexes with the nonoxidized (**L²** and **L³**) and oxidized (**L⁴** and **L⁵**) conjugates, aiming to compare their in vitro behavior in cell lines expressing or not expressing the GRPr. We expected that the biological evaluation of the ^{99m}Tc complexes would clarify if oxidation took place on the methionine residue, a crucial point for the biospecificity of the compounds chosen for this study.

The synthesis of the ^{99m}Tc(I) tricarbonyl complexes, **Tc²**–**Tc⁵**, was done by a ligand-exchange reaction of *fac*-[^{99m}Tc(H₂O)₃(CO)₃]⁺ in aqueous solution with the respective conjugates, at 100 °C for 30 min and pH 7.4 (Scheme 2). The chemical identity of **Tc²**–**Tc⁵** was confirmed by comparison of their HPLC profiles with the ones of the corresponding Re complexes **Re²**–**Re⁵** (Fig. S2, Table S2). **Tc²**–**Tc⁵** were also used to determine the respective lipophilicity of the conjugates by measurement

of the log $P_{o/w}$ values (*n*-octanol/0.1 M PBS, pH 7.4). These new conjugates are relatively hydrophilic, with log $P_{o/w}$ values spanning from −0.68 to −1.91 (Table S2).

Biological studies: cellular and nuclear uptake of the Re and ^{99m}Tc complexes

Taking advantage of the fluorescence properties of the AO intercalator, we evaluated live-cell uptake of BBN conjugates **Re²** and **Re³** by time-lapse confocal microscopy imaging. For comparison, identical studies were also performed for the Re complex bearing only an AO intercalator (**Re-AO**) (Fig. 1). As seen in Fig. 2, all of the conjugates internalize in PC3 cells, being observed as a considerable accumulation of fluorescence in the nucleus, particularly in the nucleoli (Figs. 2, S3). The model conjugate, **Re-AO**, demonstrated a faster kinetic uptake as compared with the BBN-containing analogues **Re²** and **Re³**. The fluorescence emitted from the nucleus is more intense for **Re³** than for **Re²**, which indicates a greater nuclear accumulation of the AO chromophore in the case of **Re³**. The live-cell uptake of the oxidized complex **Re⁵** was also studied by time-lapse confocal microscopy imaging. Unlike the nonoxidized congener **Re³**, **Re⁵** was unable to internalize into the PC-3 cells as almost no fluorescence was detected inside the cells (Fig. S4).

To quantify the cellular and nuclear internalization, we studied the behavior of the congener complexes **Tc²** and **Tc³** in PC3 and B16F1 cell lines. The behavior of these radioconjugates was evaluated in these two cell lines to gain some insight into the contribution of the receptor-mediated mechanism, as GRPrs are expressed by PC3 cells but not by B16F1 cells. The oxidized species **Tc⁴** and **Tc⁵** were also evaluated. Before performing in vitro cell studies, we evaluated the stability of **Tc²**–**Tc⁵** in the cell culture media by TLC. The HPLC-purified radiocomplexes were incubated with RPMI medium (PC3) and DMEM (B16F1) at 37 °C, and then aliquots were removed at different time points and evaluated by TLC. All radiocomplexes proved to be stable in both cell media during the 3-h incubation period.

The cellular internalization of complexes **Tc²**–**Tc⁵** at 37 °C was time-dependent in both cell lines (Fig. 3). **Tc²** and **Tc³** showed a higher uptake in PC3 cells (12.6 ± 1 and 17.9 ± 0.3% at 4 h incubation, respectively) when compared with the values of 8.08 ± 0.3 and 5.46 ± 0.11% found in B16F1 cells at the same time point. In comparison with **Tc²** and **Tc³**, the oxidized complexes **Tc⁴** and **Tc⁵** have a much lower uptake in PC3 cells, with only 2.29 ± 0.03 and 3.90 ± 0.3% internalized activity after 4 h of incubation, respectively. Contrastingly, the internalization of **Tc⁴** and **Tc⁵** by B16F1 cells is quite similar to that observed for **Tc²** and **Tc³** in the same cell line. Together, these data point out that the internalization of
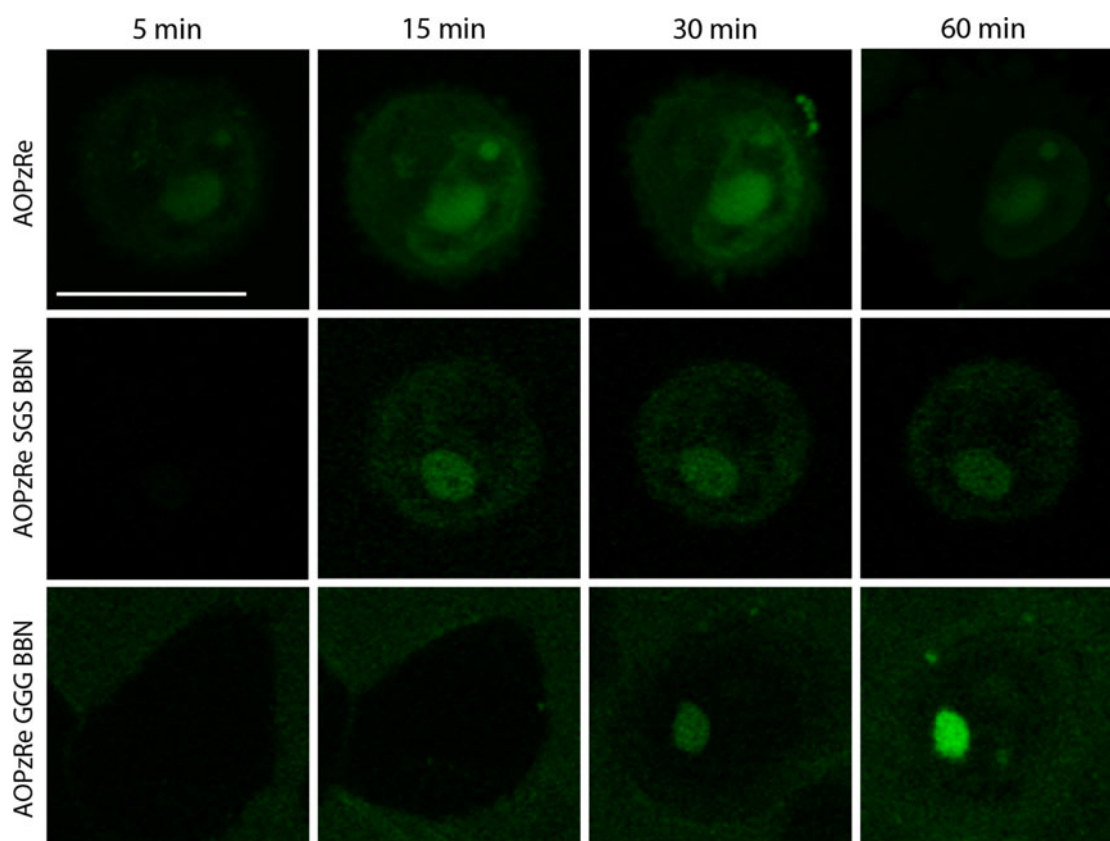
Fig. 2 Live-cell uptake of complexes **Re-AO** (*AOPzRe*), **Re²** (*AOPzRe SGS BBN*), and **Re³** (*AOPzRe GGG BBN*), visualized by time-lapse confocal microscopy imaging. PC3 cells were incubated with dihydroethidium for whole-cell staining and imaged every minute for 1 h after addition of 15 μM fluorescent Re complexes to the cell medium. Images acquired at time points of 5, 15, 30, and 60 min are shown. The results show single cell fluorescence distributions of green fluorescent Re complexes for the same time points. *Bar* 20 μm

Tc² and **Tc³** by the PC3 cells involves a receptor-mediated mechanism, as evidenced by the higher uptake in this cell line. Nevertheless, we cannot rule out the contribution of nonspecific uptake mechanisms because of the observed accumulation of activity in the GRPr-negative cell line. Along with the model complex ^{99m}Tc-AO (Fig. 1), conjugates **Tc⁴** and **Tc⁵** display a relatively similar uptake in each cell line, confirming that **Tc⁴** and **Tc⁵** lack specificity, a result which seems to indicate oxidation of the C-terminal methionine amino acid. In fact, the Q-W-A-V-G-H-L-M-NH₂ (BBN) peptide sequence is crucial in the GRPr recognition, interaction, and internalization mechanisms [26].

Owing to low cellular uptake of complexes **Tc⁴** and **Tc⁵**, only the cellular retention of complexes **Tc²** and **Tc³** was evaluated at different time points, after 1 h of internalization. A similar and moderate time-dependent externalization was found for these conjugates in both PC3 and B16F1 cells (Fig. S5).

For **Tc²**–**Tc⁵**, studies with B16F1 and PC3 cells were also performed to evaluate the accumulation of activity in the nucleus (Fig. 3). These studies consisted in the measurement of the activity retained in the nucleus fraction and outside the nucleus after lysis of the cell membrane and separation of the nucleus pellet by centrifugation [16]. The nuclear uptake was expressed as a percentage of the total activity added to the cells. The complexes exhibited nuclear internalization of less than 5% after 4 h of incubation, with the exception of **Tc³**, which showed an uptake of 10.4 ± 0.4% in the PC3 cell nucleus at the same time point. The activity in the nucleus was particularly low for the oxidized complexes **Tc⁴** and **Tc⁵** in the PC3 cell line, with internalization values of only 0.5 ± 0.01 and 0.9 ± 0.1% after 4 h of incubation, respectively. In B16F1 cells, conjugate **Tc²** had the highest nuclear internalization, with a value of 4.1 ± 0.1% at 4 h incubation, followed by **Tc⁴** (3.5 ± 0.2%), **Tc³** (2.8 ± 0.03%) and **Tc⁵** (2.0 ± 0.2%) for the same time point. Unlike the cellular uptake, this trend is not due to the presence of oxidized methionine, but certainly reflects other differences in the physicochemical properties of these radiopeptides.

The nuclear internalization of complexes **Tc²** and **Tc³** was also expressed as the ratio of radioactivity in the nucleus and that remaining in the cytoplasm (Fig. 4). As can be seen in Fig. 4, the studies performed with **Tc³** show

Fig. 3 Cellular internalization of Tc^2–Tc^5 and Tc-pz-GGG-BBN (pz is pyrazolyl and BBN is bombesin) and nuclear uptake at 37 °C in B16F1 (*left*) and PC3 (*right*) cells expressed as a percentage of total activity (mean ± standard deviation, $n = 3$)
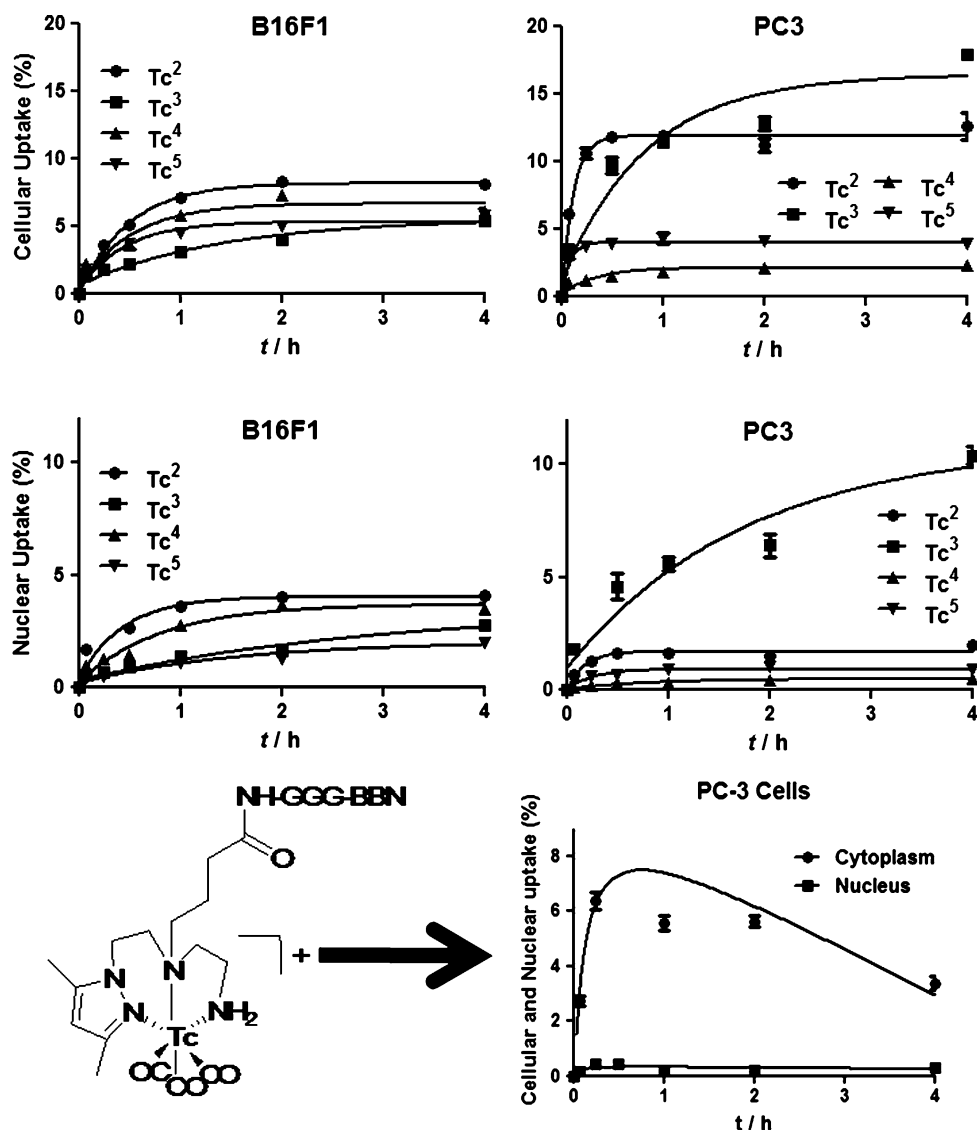
a very rapid accumulation of activity in the PC3 cell nucleus and, for all time points considered, the values are similar to those in the cytoplasm. On the other hand, for Tc^2, the percentage inside the nucleus was always significantly lower than that found in the cytoplasm. These findings are consistent with the results of the live-cell microscopy studies that showed a more pronounced accumulation of fluorescence in the nucleus for Re^3 compared with Re^2 (Figs. 2, S3). In B16F1 cells, the differences in the nuclear internalization found in the studies with Tc^2 and Tc^3 are not as striking as they were in the PC3 cell line. For Tc^2, the percentage of activity in the nucleus of B16F1 cells is similar to that outside for all time points. In this cell line and for Tc^3, the percentage found in the nucleus is also significant, ranging between 37 and 52%.

Once inside the cell, radiopeptides Tc^2 and Tc^3 are expected to be degraded in the lysosomes. The remarkably higher nuclear uptake of Tc^3 over Tc^2 in the PC3 cell line

may be due to a more extensive metabolization of Tc^3 inside the cell, favoring the nuclear targeting driven by the presence of the AO intercalator. To gain further insight into the possible role of the intercalator in the nuclear targeting ability of Tc^3, we also measured the nuclear internalization of the congener radiopeptide without the AO fragment (^{99m}Tc-pz-GGG-BBN), which has been previously reported by our group [22, 30]. ^{99m}Tc-pz-GGG-BBN showed negligible nuclear uptake (less than 0.5%) (Fig. 4), pointing out that the incorporation of the AO intercalator in the pyrazolyl-diamine framework enhances the nuclear targeting ability of the respective BBN metalloconjugates.

Conclusion

We have described novel multifunctional Re/^{99m}Tc tricarbonyl conjugates bearing a pyrazolyl-diamine framework
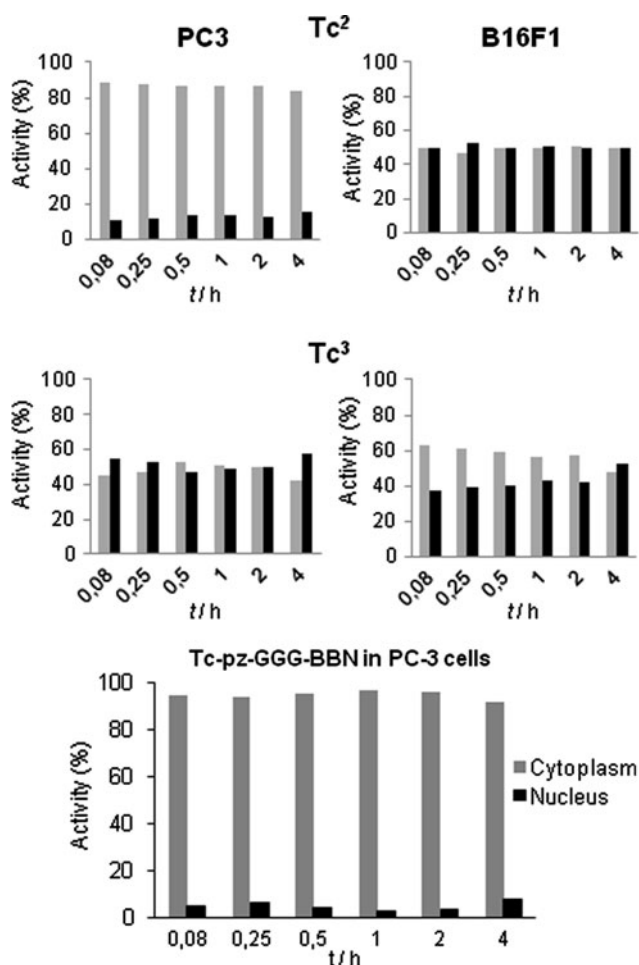
Fig. 4 Activity inside the nucleus (*black*) and in the cytoplasm (*gray*) expressed as a percentage of the internalized activity for complexes **Tc²**, **Tc³**, and Tc-pz-GGG-BBN at 37 °C in PC3 (*left*) and B16F1 (*right*) cells (mean ± standard deviation, $n = 3$)

to stabilize the metal, an AO derivative as a DNA intercalating unit and to follow the internalization and subcellular trafficking of the compounds by confocal fluorescence microscopy, and BBN peptides for specific cell targeting.

Cell uptake studies have shown that the presence of the AO intercalator and metallation with the *fac*-[M(CO)₃]⁺ (M is Re, ⁹⁹ᵐTc) core did not compromise the capability of the BBN metalloconjugates, **Re²/Tc²** and **Re³/Tc³**, to accumulate in GRPr-positive PC3 human prostate tumor cells. Parallel experiments with the corresponding oxidized complexes **Tc⁴** and **Tc⁵** and/or with B16F1 cells indicated that the cell uptake of **Re²/Tc²** and **Re³/Tc³** involves a receptor-mediated mechanism.

Of the ⁹⁹ᵐTc complexes conjugates evaluated, **Tc³**, functionalized with GGG-BBN[7-14] peptide (**10**), showed the highest cellular internalization in GRPr-positive PC3 cells, presenting enhanced nuclear uptake compared with the congener **Tc²**. Live-cell confocal imaging microscopy studies with the congener **Re³** showed a considerable

accumulation of fluorescence in the nucleus with kinetics of uptake similar to that exhibited by **Tc³**. These results show that AO and the metal fragment are colocalized in the nucleus, pointing out that they remain connected despite the lysosomal degradation of the bioactive peptide.

To the best of our knowledge, the compounds reported herein are the first examples of ⁹⁹ᵐTc bioconjugates that combine specific cell targeting with nuclear internalization, which are crucial issues in the potential usefulness of ⁹⁹ᵐTc in Auger therapy. The radiotoxicity of these ⁹⁹ᵐTc(I) tricarbonyl conjugates towards different tumor cell lines is currently under evaluation, as is their functionalization with nuclear localizing sequences to further enhance their nuclear uptake in target cancer cells.

References

1. Adam MJ, Wilbur DS (2005) Chem Soc Rev 34:153–163
2. Kassis AI, Walicka MA, Adelstein SJ (2000) Acta Oncol 39:721–726
3. Stepanek J, Ilvonen SA, Lampinen JS, Savolainen SE, Välimäki PJ, Kuronun AA (2000) Acta Oncol 39:667–671
4. Chen P, Wang J, Hope K, Jin L, Dick J, Cameron R, Brandwein J, Minden M, Reilly RM (2006) J Nucl Med 47:827–836
5. Edel S, Terrissol M, Peudon A, Kümmerle E, Pomplun E (2006) Radiat Prot Dosim 122:136–140
6. Ickenstein LM, Edwards K, Sjöberg S, Carlsson J, Gedda L (2006) Nucl Med Biol 33:773–783
7. Michel RB, Rosario AV, Andrews PM, Foldenberg DM, Mattes MJ (2005) Clin Cancer Res 11:777–786
8. Bailey KE, Constantini DL, Cai Z, Scolland DA, Chen Z, Reilly RM, Vallis KA (2007) J Nucl Med 48:1562–1570
9. Häfliger P, Agorastos N, Spingler B, Georgiev O, Viola G, Alberto R (2005) ChemBioChem 6:414–421
10. Agorastos N, Borsig L, Renard A, Antoni P, Viola G, Spingler B, Kurz P, Alberto R (2007) Chem Eur J 13:3842–3852
11. Zelenka K, Borsig L, Alberto R (2011) Org Biomol Chem 9:1071–1078
12. Schipper ML, Riese CG, Seitz S, Weber A, Behe M, Schurrat T, Schramm N, Keil B, Alfke H, Behr TM (2007) Eur J Nucl Med Mol Imaging 34:638–650
13. Chan CR, Cai ZL, Su RF, Reilly RM (2010) Nucl Med Biol 37:105–115
14. Vitor RF, Correia I, Videira M, Marques F, Paulo A, Pessoa JC, Viola G, Martins GG, Santos I (2008) ChemBioChem 9:131–142
15. Vitor RF, Esteves T, Marques F, Raposinho P, Paulo A, Rodrigues S, Rueff J, Casimiro S, Costa L, Santos I (2009) Cancer Biother Radiopharm 24:551–563
16. Esteves T, Xavier C, Gama S, Mendes F, Raposinho PD, Marques F, Paulo A, Pessoa JC, Rino J, Viola G, Santos I (2010) Org Biomol Chem 8:4104–4116

17. Smith CJ, Volkert WA, Hoffman TJ (2005) Nucl Med Biol 33:733–740
18. Perrin DD, Armarego WL (1988) Purification of laboratory chemicals, 3rd edn. Pergamon Press, Oxford
19. Lazarova N, James S, Babich J, Zubieta J (2004) Inorg Chem Commun 7:1023–1026
20. Moura C, Esteves T, Gano L, Raposinho PD, Paulo A, Santos I (2010) New J Chem 34:2564–2578
21. Merrifield RB (1985) J Am Chem Soc 85:2149–2154
22. Alves S, Paulo A, Correia JDG, Gano L, Smith CJ, Hoffman TJ, Santos I (2005) Bioconjug Chem 16:438–449
23. Troutner DE, Volkert WA, Hoffman TJ, Holmes RA (1984) Int J Appl Radiat Isot 35:467–470
24. Abney JR, Cutler B, Fillbach ML, Axelrod D, Scalettar BA (1997) J Cell Biol 137:1459–1468
25. Smith CJ, Sieckman GL, Owen NK, Hayes DL, Mazuru DG, Kannan R, Volkert WA, Hoffman TJ (2003) Cancer Res 63:4082–4088
26. Vogt W (1995) Free Radic Biol Med 18:93–105
27. Smith CJ, Gali H, Sieckman GL, Higginbotham C, Volkert WA, Hoffman TJ (2003) Bioconjug Chem 14:93–102
28. Zhang H, Chen J, Waldherr C, Hinni K, Waser B, Reubi JC, Maecke HR (2004) Cancer Res 64:6707–6751
29. Vigna SR (1989) Biol Bull 177:192–194
30. Alves S, Correia JDG, Santos I, Veerendra B, Sieckman GL, Hoffman TJ, Rold TL, Figueroa SD, Retzloff L, McCrate J, Prasanphanich A, Smith CJ (2006) Nucl Med Biol 33:625–634